Spatial Channel Cross-Connect Architectures for Spatial Channel Networks

Masahiko Jinno, *Fellow, IEEE*

(Invited Paper)

***Abstract*—A spatial channel network (SCN) is a novel optical network architecture targeting the space division multiplexing (SDM) era where the optical layer is explicitly evolved into the hierarchical SDM layer and wavelength division multiplexing layer, and an optical node is decoupled into a spatial channel cross-connect (SXC) and a wavelength cross-connect to form a hierarchical optical cross-connect. In this article, we discuss a wide variety of SXC architectures based on optical matrix switches (MSs) and newly proposed core selective switches (CSSs) from the viewpoints of connection flexibility and architectural complexity. After briefly reviewing the architecture and functionalities of an SCN and its building-block optical devices, novel SXC architectures based on sub-MSs and CSSs are described and formulas are derived for each SXC architecture that give the required number of optical devices, switching mirrors, and internal fiber connections. Based on the formulations, these architectures are compared with traditional SXC architectures based on a high-port count full-MS pair and a Clos network from the viewpoints of the freedom of connection functionalities, operational benefits, and potential node costs associated with the architectural complexity in order to obtain insights regarding which network application is suited to each SXC architecture.**

***Index Terms*—Spatial division multiplexing (SDM), wavelength division multiplexing, spatial channel, spatial bypass, spatial cross-connect, matrix switch, core selective switch.**

GLOSSARY

AC	Any-core access
BoL	Beginning of life
ClL	Colorless
CnL	Contentionless
CS	Core selector
CSS	Core selective switch
CPS	Core/port selector
D	Directional
EoL	End of life
FC	Fixed-core access
HOXC	Hierarchical optical cross-connect
LC	Lane change
MCF	Multicore fiber
MEMS	Micro electro-mechanical systems
MS	Matrix switch
ND	Non-directional
NLC	Non-lane change
OCh	Optical channel
OH	Overhead information
OMS	Optical multiplexing section
OTN	Optical transport network
R&S	Route and select
RCA	Routing and core assignment
ROADM	Reconfigurable optical add drop multiplexer
SCh	Spatial channel
SCN	Spatial channel network
SDEMUX	Spatial demultiplexer
SDM	Space division multiplexing
SL	Spatial lane
SMF	Single mode fiber
SMS	spatial multiplexing section
SMUX	Spatial multiplexer
SXC	Spatial channel cross-connect
WC	Wavelength conversion
WDM	Wavelength division multiplexing
WSS	Wavelength selective switch
WXC	Wavelength cross-connect

Manuscript received November 6, 2019; revised January 15, 2020; accepted January 22, 2020. Date of publication February 21, 2020; date of current version April 13, 2020. This work was supported in part by the JSPS KAKENHI under Grants 26220905 and JP18H01443 and in part by the National Institute of Information and Communication Technology (NICT) under Grants 19302 and 20401.

The author is with the Faculty of Engineering and Design, Kagawa University, Takamatsu 761-0396, Japan (e-mail: jinno@eng.kagawa-u.ac.jp).

Color versions of one or more of the figures in this article are available online at http://ieeexplore.ieee.org.

Digital Object Identifier 10.1109/JSTQE.2020.2975660

I. INTRODUCTION

BASED on the extrapolation of recent compound annual growth rates of high-end router blades, which is at approximately 40%, and other technologies used to generate and process data, Drs. Winzer and Neilson recently predicted that commercial 10-Tb/s optical interfaces working in 1-P b/s optical transport systems will be needed by around 2024 [1], [2]. Since the optical-transport system capacity of 1-P b/s far exceeds the fundamental capacity limit of the conventional single mode fiber (SMF), which is considered to be approximately 100 Tb/s, there will be massive numbers of SMFs and/or novel fibers with new core structures that support multiple guided spatial modes between adjacent optical nodes. An uncoupled single-mode multicore fiber (MCF) is one such new core-structure fiber in which multiple uncoupled single-mode cores are placed within a single fiber cladding [3]. An uncoupled MCF has advantages over other new core-structure fibers such as a multimode fiber

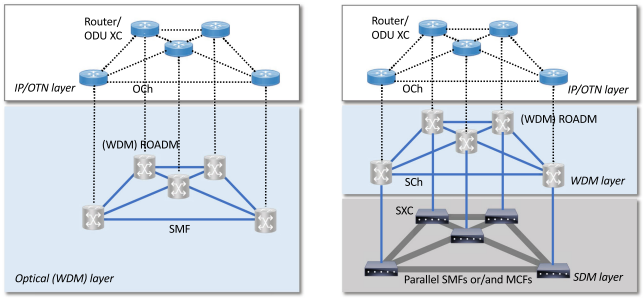

(a) Current WDM network (b) Possible optical network in SDM era

Fig. 1. Envisioned optical network evolution toward SDM abundant era. The optical layer can evolve into hierarchical WDM and SDM layers and an optical node can be decoupled into a potentially low-loss SXC and a conventional WXC to achieve a hierarchical optical cross-connect.

or a coupled core multicore fiber, especially for medium-haul terrestrial networks, because it is compatible with the current SMF-based transmission technologies in terms of not requiring complicated multiple-input multiple-output (MIMO) digital signal processing (DSP) for spatial demultiplexing. So, a near or middle-term solution for the capacity crunch of current SMFs, at least in terrestrial networks, would be to use parallel SMFs and/or uncoupled MCFs.

So far, considerable research efforts have been dedicated to achieving larger scale single-layer reconfigurable optical add drop multiplexers (ROADMs) or wavelength cross-connects (WXCs) toward the forthcoming space division multiplexing (SDM) era. Such efforts include joint switching of a spatial superchannel where a single switching element is shared among constituting spatial sub-channels [4]–[7]. Another example is a subsystem-modular WXC in which multiple small-scale sub-WXCs are connected via a limited number of intra-node SMFs [8], [9]. Note that they are designed to be used in single-layer wavelength division multiplexing (WDM) networks and to handle traffic demands only at fine wavelength granularity. However, since optical channels having bit rates of 10-Tb/s and beyond that will be needed by around 2024 will occupy almost the entire available spectrum in a conventional SMF, it is quite clear that for such a ultra-high capacity optical channel (OCh), the wavelength switching layer is no longer necessary.

Considering the above-noted trend in optical transport systems and recalling the introduction of an optical bypass when entering the wavelength abundant era in the early 2000s [10], [11], it would be natural to consider introducing a *spatial bypass* through a spatial channel cross-connect (SXC) rather than working on achieving larger scale single-layer ROADMs or WXCs [4]–[9], [12], [13] in the forthcoming SDM era. In this scenario, the optical layer should evolve into hierarchical WDM and SDM layers as shown in Fig. 1. Along with this, an optical node should be decoupled into a potentially low-loss SXC and a conventional WXC to achieve a hierarchical optical cross-connect (HOXC). This will support a wide variety of traffic demands from the wavelength level to spatial level in a cost-effective manner and to yield prominent extension of the optical reach for spatially bypassed OChs.

The idea of a hierarchical (or multi-granular) optical network with a coarser granular but more cost-effective switching layer(s) than the wavelength layer, *e.g.*, wavelength band and fiber layers, is not new at all. Since its proposal at the end of the 1990s [14]–[16], there have been considerable research efforts in this area [17], [18]. However, in our opinion, hierarchical optical networks have remained rather marginal even after spatial division multiplexing (SDM) technology began to attract much attention [19]–[22]. As far as we know, there is no report that has focused on practical issues such as the growability, reliability, techno-economics, and fiber-to-fiber insertion loss characteristics of hierarchical optical node architectures.

According to these observations, we recently reevaluated traditional hierarchical (or multiglandular) optical networks and proposed a *spatial channel network* (SCN) architecture for the SDM layer that employs a *spatial bypass* through a potentially low-loss SXC [23], [24]. In an SCN, a spatial channel (SCh) is defined as an ultra-high capacity optical data stream that is allowed to occupy the entire available spectrum of, for example, a core in an SMF or an MCF. If there is a single or aggregate traffic flow that is sufficiently large to fill almost the entire bandwidth of an SCh between the source and destination nodes, an SCh, which bypasses the overlying WDM layer, is established between them. If there is an insufficient amount of traffic between a source/destination pair, the corresponding OCh shares an SCh with other low capacity OChs having different source/destination pairs by using a WXC to achieve better spatial resource utilization [24]. This relationship between an SXC and a WXC is very similar to the current hierarchical IP (over OTN) over WDM network shown in Fig. 1(a). In this case, an OCh is established between a source/destination pair where a sufficient amount of traffic to fill almost the entire capacity of the wavelength exists, and the sub-wavelength grooming is performed in the overlying OTN or IP layers using an ODU-XC or an IP router.

If we employ the traditional approach, a possible SXC architecture would be based on an $N \times N$ optical matrix switch (MS) connected in parallel to the secondary MS with optical splitters and optical 2×1 switches or $N \times M$ MSs configured to achieve a Clos network. Both configurations are strictly non-blocking, however, their requirements for optical matrix switches are challenging. The former requires two ultra-high port count optical MSs in the order of $CD \times CD$, where C is the number of single mode cores per link and D is the node degree, while the latter requires a large number of moderate size $(\sim C \times 2C)$ MSs in the order of $2(C + D)$.

In order to address the above problem in non-blocking SXCs, we proposed two types of growable and reliable SXC architectures based on a sub-MS and a *core selective switch* (CSS) [23]–[28]. Both architectures are designed to reduce the node complexity at the expense of introducing a reasonable connection constraint. The former is a moderate size MS formed by dividing a full-size MS, while the latter is an SDM counter part of the conventional wavelength selective switch (WSS). The idea behind these approaches is based on introducing connection constraints considering the fact that all spatial lanes (SLs) in an SDM link are directed to the same adjacent node. This leads

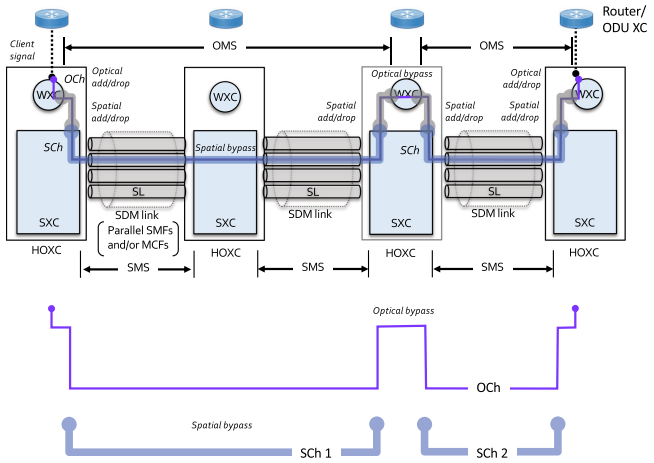

Fig. 2. Spatial channel network (SCN) architecture. An SDM link comprises multiple SLs whose physical entities are single mode cores in parallel SMFs and/or parallel MCFs. An SXC performs SL level multiplexing and grooming and serves as the main switch at an HOXC.

to employing less complicated and consequently cost-effective optical switches.

In [23] and [24], we only showed the conceptual diagrams for the two proposed types of SXC architectures with a simple add drop part and the preliminary cost evaluation results for each architecture. Clearly, there must be a wide variety of add/drop part architectures and technologies to achieve a flexible add/drop part in an SXC with functionalities that correspond to *colorless* (ClL), *non-directional* (ND), which is often referred to as *directionless*, and *contentionless* (CnL) features and the wavelength conversion (WC) capability in current ROADMs. Since such connection flexibilities are associated with additional cost and so different network operators or over-the-top players may have different preferences, we must establish technology options in the SXC design that meets individual requirements at a reasonable cost and insertion loss.

In this paper, we discuss detailed SXC architectures based on MSs and CSSs from the viewpoints of connection flexibility and architectural complexity. The remaining part of this paper is structured as follows: In Section II, the SCN architecture is reviewed and the connection functionality definitions in an SXC used in the following sections are given. In Sections III and IV, detailed SXC architectures based on MSs and CSSs and their building-block optical devices are described. Formulations that give the required numbers of optical devices, switching mirrors, and internal fiber connections for each SXC architecture are also derived. Finally, these architectures are compared and analyzed from the viewpoints of the freedom of connection functionalities and architectural complexity.

II. SCN Architecture

A. SCN Architecture

Fig. 2 shows the SCN architecture [24]. In the SDM layer, the architecture comprises SDM links and SXCs. An SDM link comprises multiple SLs whose physical entities are single mode

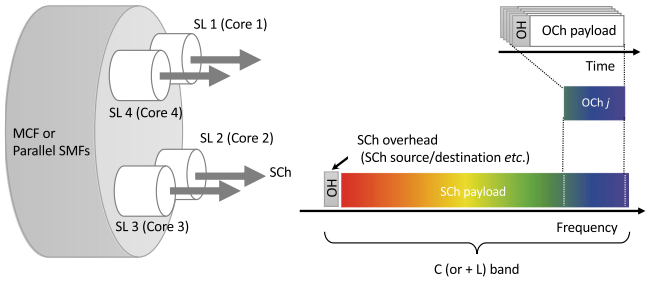

Fig. 3. Spatial channel (SCh) structure. An SCh transports a single or multiple OChs that are spectrally aligned with the flexible grid paradigm.

cores in parallel SMFs and/or parallel MCFs. In an SDM link, each SL may be labeled with its identification number. An SXC performs SL level multiplexing and grooming and serves as the main switch at an HOXC. In the WDM layer, a WXC performs wavelength level multiplexing and grooming and serves as an edge switch at an HOXC. Following the definition of the optical multiplexing section (OMS) in a current optical transport network (OTN), which is defined between adjacent WXCs, a *spatial multiplexing section* (SMS) is defined between adjacent SXCs.

B. Spatial Channel Structure

An SCh transports a single or multiple OChs that are spectrally aligned with the G.694.1 flexible grid paradigm as shown in Fig. 3. An SCh may include its in-band overhead information (SCh OH) such as source/destination node identification numbers and is spatially routed end to end as a single entity through SXCs bypassing the overlying WDM layer. If there is a single or aggregate traffic flow that is sufficiently large to fill almost the entire bandwidth of an SCh between the source and destination nodes, an SCh is established between them. Such SChs bypass the overlying WDM layer (*spatial bypass*). If there is an insufficient amount of traffic between a source/destination pair, the corresponding OCh shares an SCh with other low-capacity OChs that have different source/destination pairs for better spatial resource utilization. An SCh comprises SLs with the same or different identification numbers depending on the *lane change* capability of SXCs on the route.

C. Requirements for SXC

As described in [24] and [29], a requirement for practical SXCs from the viewpoint of physical performance is that the SXC insertion loss must be sufficiently low to not degrade the transmission performance of OChs that are spectrally groomed by a WXC. Gaussian noise model [30] analysis revealed that if we assume, for example, a 20-dB transmission loss per link and a 20-dB insertion loss per WXC, an SXC with an insertion loss of less than 7 dB can provide an optical reach for spectrally groomed OChs that is more than 95% of that for an OCh transported through a conventional single-layer WDM network [29]. From an operational point of view, a requirement for practical SXCs is reliability based on the design policy to ensure no single point of failure or small failure group. Growability in terms of the

TABLE I
PARAMETERS USED FOR COMPARING SXC ARCHITECTURES

Symbol	Quantity	Value
D	Node degree	8
C	Number of single-mode cores	64
a	Add drop ratio $(0 \le a \le 1)$	0.25
s	Partitioning number of cores $(1 \le s)$	4

node degree (2 to 8), add-drop ratio (up to 50%), and number of SLs that ensures a low start-up cost and pay-as-you-grow approach is generally mandatory and especially favored in terrestrial systems.

On the other hand, the connection flexibility in the add drop part of an SXC may be optional since it is associated with additional cost and insertion loss. Strict-sense non-blocking connectivity for an SCh in an SXC can be expressed as "any core (SL) from any direction (SDM link) can be connected to any transceiver or any core of any direction". According to the terminology used in current ROADMs, *i.e.*, ClL, ND, and CnL features and the WC capability, the strict-sense non-blocking connectivity for an SCh can be decomposed into degrees of connection freedom. In the remaining part of this paper, we refer to these as *any-core access* (AC), *non-directional* (ND), *contentionless* (CnL), and a *lane-change* (LC) features, respectively.

III. MS BASED SXC ARCHITECTURES

In this section, we discuss detailed SXC architectures based on MSs and their building-block optical devices. We also derive formulas that give the required numbers of optical devices and switching mirrors for each SXC architecture as a function of node degree D, the number of single-mode cores per link C, the add drop ratio of the SXC a, and partitioning number of cores s. Values used for comparing SXC architectures are summarized in Table I. As an index to estimate relative costs of various types of switching devices, we employ the number of micro electro-mechanical systems (MEMS) mirrors used in an SXC since it increases with the node size and is considered a major part of the node cost.

A. Building Blocks for MS Based SXCs

1) Optical MS: Fig. 4(a) is a schematic diagram of an $N \times N$ MS as a building block of an MS-based SXC, which has N input SMFs and N output SMFs. An optical signal from any input SMF can be switched to any output SMF so long as there is no optical signal that has already been switched to the output SMF. Nowadays, a wide range of MSs with the size of 4×4 to more than 300×300 employing either MEMS mirrors or SMF collimators mounted on piezoelectric actuators are commercially available. Such commercial MSs are based on free-space optics and exhibit very low insertion loss of less than 1 dB to approximately 2 dB depending on the switch size. The required number of MEMS mirrors or piezoelectric actuators per MS increases as $2N$.

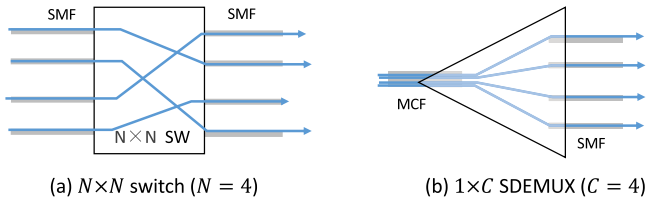

Fig. 4. Building blocks for matrix switch based SXCs. An $N \times N$ MS has N input SMFs and N output SMFs. An SDEMUX has a one-input MCF and C-output SMF when it is used as an SDEMUX.

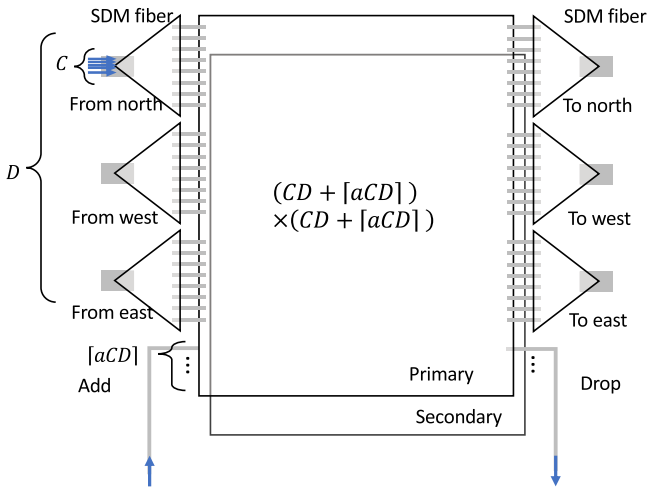

Fig. 5. Architecture of full MS based SXC (strict-sense non-blocking). D input MCFs that support C cores and D output MCFs are connected on each side of an $N \times N$ MS via a $1 \times C$ SDEMUX and a $C \times 1$ SMUX, where $N = CD + aCD$ and $\lceil \cdot \rceil$ denote the ceiling function and a denotes the drop ratio.

2) Spatial Multiplexer/Demultiplexer (SMUX/SDEMUX): When input and output SDM fibers are MCFs, another type of optical device, a spatial multiplexer/demultiplexer (SMUX/SDEMUX), is required. It has a one-input MCF and C-output SMF (when it is used as an SDEMUX) as shown in Fig. 4(b). An optical signal from the n-th core of the input MCF is output to the n-th output SMF. So far, various types of SMUX/SDEMUX have been reported. For example, fiber-bundle type compact SMUXs/SDEMUXs for a 7-core MCF with the insertion loss of <0.3 dB [31] and for a 19-core MCF with the insertion loss, total crosstalk, length, and outer diameter of <1.15 dB, <-59 dB, 15 mm, and 2 mm, respectively [32], were reported.

B. Full-MS Based Configuration

Fig. 5 shows a strict-sense non-blocking SXC architecture based on high-port-count $N \times N$ MSs where $N = CD + aCD$ and $\lceil \cdot \rceil$ denotes the ceiling function. Here, D input MCFs that support C cores and D output MCFs are connected on each side of the MS via a $1 \times C$ SDEMUX and a $C \times 1$ SMUX. If $D = 8$,

TABLE II
REQUIRED DEVICES FOR FULL MATRIX SWITCH BASED SXC (NON-BLOCKING) SHOWN IN FIG. 5

Device		Input/output port count		Number of mirrors per device		Number of devices	Total number of mirrors	
MS	EoL	$(CD+\lceil aCD\rceil)$ $\times(CD+\lceil aCD\rceil)$	640 $\times$640	$2(CD$ $+\lceil aCD\rceil)$	1280	2	$4(CD+\lceil aCD\rceil)$	2560
	BoL					↑	↑	

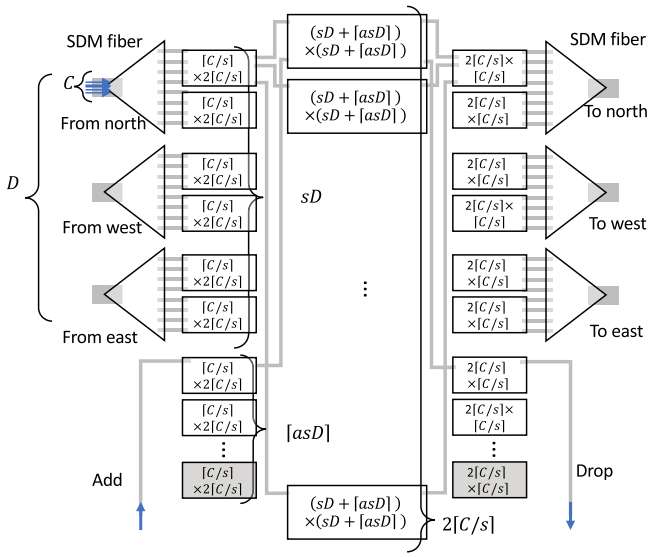

Fig. 6. Architecture of Clos network based SXC (strict-sense non-blocking), where the required port count per MS in the full-MS based SXC architecture can be reduced at the expense of increased numbers of comprising moderate-sized MSs, total mirrors, and intra-SXC wiring.

$C=64$, and $a=0.25$, we need ultra-high port count 640×640 MSs. Here, aCD $(=128)$ ports per side in the MS are for add/drop traffic where add and drop SChs are directly connected via SMFs. Preparing for an MS failure, primary and secondary high port count MSs that are connected in parallel to each other with an optical 2×1 switch pair are implemented. When the primary MS fails, an optical 2×1 switch that accommodates the affected SChs switchovers the connection to the secondary MS. When a link along the working SCh fails, MSs at the endpoints of the working SCh reroute the connection to a diverse route. The required number of mirrors per MS is 1,280 $(=2N)$. In this architecture, we need two $(CD+aCD)\times(CD+aCD)$ MSs at the beginning of life (BoL) even if the initial traffic volume is low and the required total number of mirrors per SXC becomes $4N$ $(=2,560)$. These results are summarized in Table II.

C. Clos Network Based Configuration

If a Clos network, which is a three-stage switching network as shown in Fig. 6, is employed, the required port count per MS in the full-MS based SXC architecture can be reduced at the expense of increased numbers of comprising moderate-sized MSs, total mirrors, and intra-SXC wiring. It is strict-sense non-blocking if the number of center switches m is $\geq 2n-1$ where n is the input port count of the ingress stage MS. The size of the ingress stage MS per MCF can be reduced by partitioning cores into s core groups. By choosing working and backup routes so that they are SDM link disjoint, ingress (egress) stage MS disjoint, and center stage MS disjoint from each other, this architecture supports fault-independent protection, which covers both an SDM link failure and an MS failure without any extra switch resources for equipment protection. In Fig. 6, MSs indicated by the white squares including two ingress- and egress-stage MS pairs for the path protection are required at BoL for the initial traffic demand, while the MS add/drop part indicated by the gray squares are added as a traffic demand increase. In this architecture, we need a large number of MSs: $2(sD+asD)$ $(=80)$ ingress/egress MSs with a size of $(C/s)\times(2C/s)$ $(=16\times32)$ and $2C/s$ $(=32)$ center MSs with a size of $(sD+asD)\times(sD+asD)$ $(=40\times40)$ at the end of life (EoL). The required number of MSs and associated mirrors at BoL and EoL are summarized in Table III.

D. Sub-MS Based Configuration

Fig. 7 shows an SXC architecture based on s sub-MSs. Here, cores in an MCF are partitioned into s core groups and each core group is accommodated in a different sub-MS with a size of $(C/sD+aCD/s)\times(C/sD+aCD/s)(=160\times160$ for $s=4$ and $=80\times80$ for $s=8)$. In this architecture, a core that belongs to a core group can only be connected to a core in a different direction or a transceiver that belongs to the same core group. Instead, this architecture achieves growability in terms of SLs and supports fault independent protection by choosing working and backup routes to be SDM link disjoint and sub-MS disjoint. Nevertheless, it requires half the total number of mirrors that the full-MS based SXC architecture requires even at EoL. Hereafter, we refer to these features (constraints) of the sub-MS based SXC as *partial any-core access* (PAC), *non-directional* (ND), contention-less (CnL), and *partial lane change* (PLC), respectively. The required number of MSs and associated mirrors at BoL and EoL are summarized in Table IV.

IV. CSS BASED SXC ARCHITECTURES

In this section, we first describe an architecture for a novel optical switch CSS, which is a key building block for reliable and growable SXCs. A CSS is a novel optical device that was proposed in [23] and [24], and is the SDM counterpart of a WSS in a current WDM network. Similarly, we need to create novel optical devices working in a CSS-based SXC providing the AC feature. As such optical devices, we describe a *core selector* (CS) and its extended version, a *core/port selector* (CPS). Following the description of the building block optical switches, we discuss a line-side architecture for a CSS-based SXC and a wide variety of client-side architectures for a CSS based SXC in terms of connection flexibility and node complexity. Using the same

TABLE III
REQUIRED DEVICES FOR CLOS NETWORK BASED SXC (NON-BLOCKING) SHOWN IN FIG. 6

Device		Input/output port count		Number of mirrors per device		Number of devices		Total number of mirrors	
Ingress/ egress MS	EoL	$(\lceil C/s \rceil) \times (2\lceil C/s \rceil)$	16 ×32	$3\lceil C/s \rceil$	48	$2(sD + \lceil asD \rceil)$	80	$6\lceil C/s \rceil (sD + \lceil asD \rceil)$	3840
	BoL					$2(sD + 2)$	66	$6\lceil C/s \rceil (sD + 2)$	3168
Center MS	EoL	$(sD + \lceil asD \rceil) \times (sD + \lceil asD \rceil)$	40 ×40	$2(sD + \lceil asD \rceil)$	80	$2\lceil C/s \rceil$	32	$4\lceil C/s \rceil (sD + \lceil asD \rceil)$	2560
	BoL					↑		↑	

TABLE IV
REQUIRED DEVICES FOR SUB MATRIX SWITCH BASED SXC (PAC/ND/CNL/PLC) SHOWN IN FIG. 7

Device		Input/output port count		Number of mirrors per device		Number of devices		Total number of mirrors	
MS	EoL	$(\lceil C/s \rceil D + \lceil aCD/s \rceil) \times (\lceil C/s \rceil D + \lceil aCD/s \rceil)$	160 ×160	$2(\lceil C/s \rceil D + \lceil aCD/s \rceil)$	320	s	4	$2s(\lceil C/s \rceil D + \lceil aCD/s \rceil)$	1280
	BoL					2		$4(\lceil C/s \rceil D + \lceil aCD/s \rceil)$	640

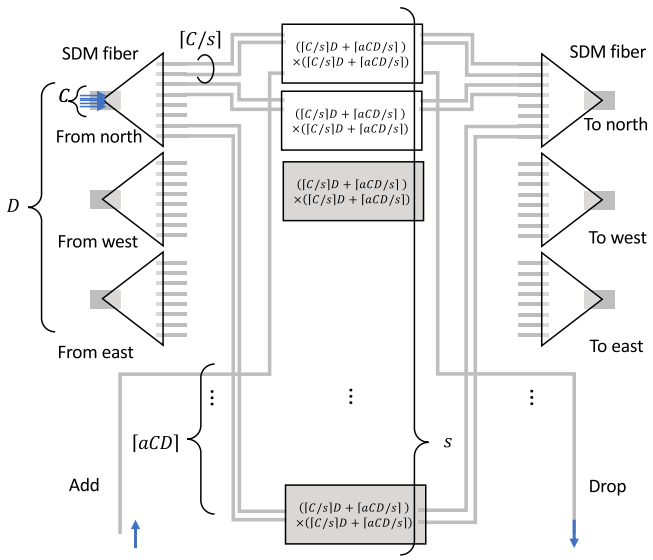

Fig. 7. Architecture of sub-matrix switch based SXC (PAC/ND/CnL/PLC). Cores in an MCF are partitioned into s core groups and each core group is accommodated in a different sub-matrix switch.

parameters, *i.e.,* node degree D, the number of single-mode cores per link C, the add drop ratio of the SXC a, and partitioning number of cores s described in Section III, we derive formulas that give the required numbers of optical devices and switching mirrors for each SXC architecture.

A. Building-Block Optical Switches for CSS Based SXCs

1) CSS: Fig. 8(a) is a schematic diagram of a $1 \times N$ CSS supporting C cores as a building block of CSS-based SXCs. It has an input MCF and N output MCFs where each MCF has C cores in its cladding. Its equivalent circuit can be expressed as shown in Fig. 8(b). Optical signals propagated through cores of the input MCF are spatially demultiplexed by a $1 \times C$ SDEMUX, launched into $1 \times N$ switches as shown in Fig. 8(c). Each optical signal is then routed and spatially multiplexed with a $C \times 1$ SMUX into its output MCFs. There is currently no commercially available CSS. Certainly, the CSS shown in Fig. 8(b) could be built using discrete optical devices; however, it would be bulky and most likely expensive. One way to achieve a compact and cost-effective CSS will be to employ free-space optics.

Fig. 9 shows the free-space-optics based architecture of a 1×4 CSS that supports four-core MCFs [25], [26]. The CSS comprises two-dimensionally arranged input and output MCFs with collimating lenses, a condenser lens, and two-dimensionally arranged switching elements. The collimating lens and condenser lens are set to form a tele-centric configuration. Four beams launched from each core of an input MCF (center) converge to the same spot at the focus of the collimating lens at different angles. A condenser lens focuses each beam on a different switching mirror according to its angle. If facets of all the output MCFs are rotationally aligned to that of the input MCF, a beam from any core of the input MCF can be connected to a core with the same index of any output MCF (periphery) by controlling the tilt of each mirror in two angular dimensions.

As described in the next subsection, since CSSs are used in the route-and-select (R&S) configuration, the horizontal flipping in the core position that occurs at an ingress CSS can be restored to the original core position by implementing the switching again at an egress CSS. After all, we can see that an SXC employing the free-space-optics based CSSs in the R&S configuration provides the connection between cores with the same index as a whole [25], [26].

Since there is most likely no need to change seamlessly the switching area, which is required for flexible-grid-enabled WSSs, MEMS mirrors that excel in terms of available larger switching angles and polarization independency may be preferable as switching elements rather than liquid-crystal-on-silicon spatial light modulators [25]. It should be noted that the free-space optics-based design of the CSS shown in Fig. 9 allows us to arrange both switching mirror elements and output MCFs in

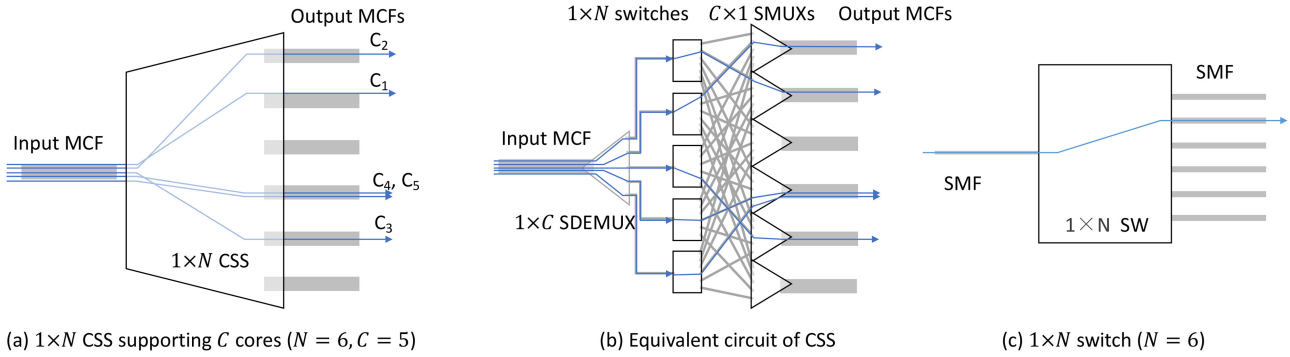

Fig. 8. Functionality and equivalent circuit of CSS, which has an input MCF and N output MCFs where each MCF has C cores in its cladding. Optical signals propagated through cores of the input MCF are spatially demultiplexed by a $1 \times C$ SDEMUX and launched into $1 \times N$ switches, whose functionality is shown in (c). Each optical signal is then routed and spatially multiplexed with a $C \times 1$ SMUX into its output MCFs.

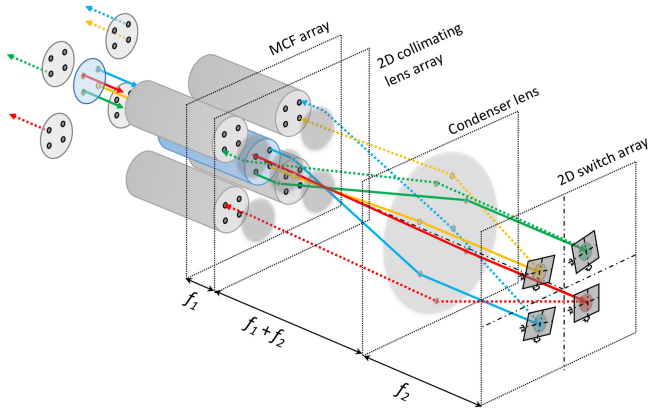

Fig. 9. Free space optics-based CSS ($N = 4$, $C = 4$). The CSS comprises two-dimensionally arranged input and output MCFs with collimating lenses, a condenser lens, and two-dimensionally arranged switching elements.

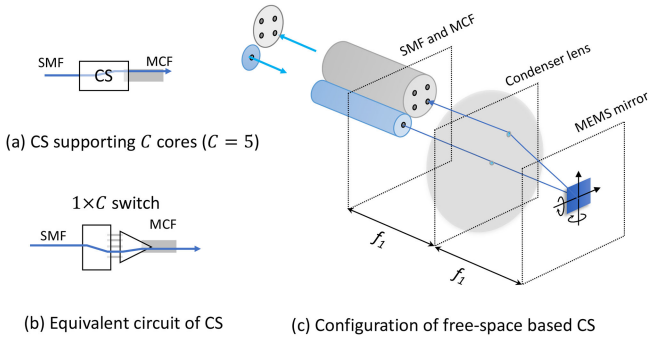

Fig. 10. Functionality, equivalent circuit, and operational principle of CS, which has an input SMF and an output MCF with C cores in its cladding. A CS can be achieved by employing very simple free-space optics comprising a condenser lens and an MEMS mirror that can be tilted in two angular dimensions.

two spatial dimensions, which yields a significant increase in the supportable number of cores (SLs) and the CSS port count.

The required number of mirrors per CSS equals C.

2) CS: Fig. 10(a) is a schematic diagram of a CS as a building block for CSS-based SXCs with the AC feature as described in the next subsection. A CS has an input SMF and an output MCF with C cores in its cladding. Its equivalent circuit can be expressed as shown in Fig. 10(b). A CS can be achieved by employing very simple free-space optics comprising a condenser lens and an MEMS mirror that can be tilted in two angular dimensions as shown in Fig. 10(c).

3) CPS: Fig. 11(a) is a schematic diagram of a $1 \times N$ CPS as a building block for CSS-based SXCs with the AC, ND, and CnL features as described in the next subsection. A CPS has an input SMF and N output MCFs with C cores in its cladding. Its equivalent circuit can be expressed as shown in Fig. 11(b). Similar to a CS, a CPS can be achieved by employing simple free-space optics comprising a condenser lens and an MEMS mirror that can be tilted in two angular dimensions.

The CS and CPS structures are very similar to that of a mature commercially available $1 \times N$ optical switch that has an input SMF and N output SMFs. Unlike a CSS, in a CS and CPS, basically no rotational alignment of the MCF facet is required. The required number of mirrors per CS and CPS is one. Nowadays, several vendors produce very compact SMF $1 \times N$ optical switches ($N \geq 8$) implemented in a cylindrical housing with a length of approximately 30 mm and a diameter of approximately 5 mm. Therefore, we may expect to achieve compact CPs and CPSs with a reasonable cost.

B. Line-Side Architecture of CSS-Based SXC

Fig. 12(a) shows the line-side architecture of a CSS-based SXC where $2D$ ingress and egress CSSs linked to MCF transmission lines are arranged in the R&S configuration instead of the *broadcast and select* (B&S) configuration in order to avoid the inherent splitting loss of an optical splitter used in the B&S configuration and to achieve a low insertion loss SXC. This is because, as reported in [24] and [28], a low insertion loss in an SXC is indispensable for achieving an optical reach for a spectrally groomed OCh in an SCN that is almost the same as the optical reach in a current WDM network. A CSS-based SXC architecture does not provide LC capability.

When adjacent SXCs are connected via parallel SMFs instead of an MCF, an SDEMUX (SMUX) is implemented between an ingress (egress) MCF and parallel SMFs as shown in Fig. 12(b).

C. Client-Side Architectures of CSS-Based SXC

1) SMUX-Type (FC/D/CnL/NLC): Fig. 13 shows an SXC architecture based on CSSs ($D = 3$, $C = 4$) that provides *fixed*

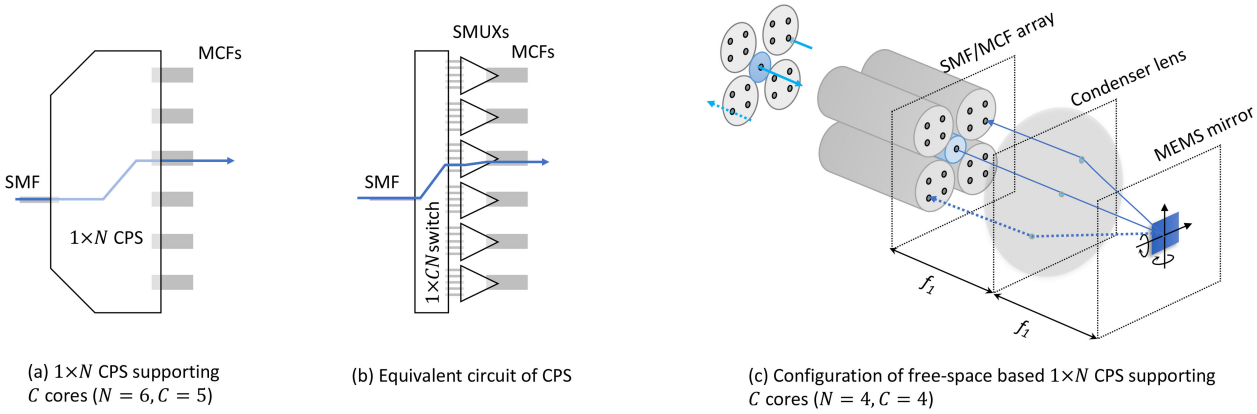

(a) $1\times N$ CPS supporting C cores ($N=6, C=5$)

(b) Equivalent circuit of CPS

(c) Configuration of free-space based $1\times N$ CPS supporting C cores ($N=4, C=4$)

Fig. 11. Functionality, equivalent circuit, and operational principle of CPS, which has an input SMF and N output MCFs with C cores in its cladding. Similar to a CS, a CPS can be achieved by employing simple free-space optics comprising a condenser lens and an MEMS mirror that can be tilted in two angular dimensions.

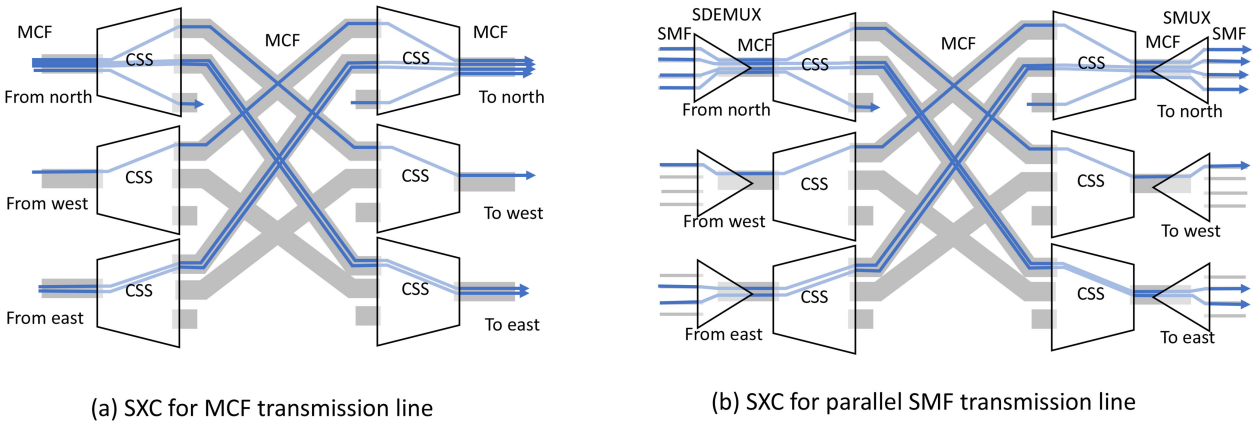

(a) SXC for MCF transmission line

(b) SXC for parallel SMF transmission line

Fig. 12. Line-side architecture of CSS-based SXC. $2D$ ingress and egress CSSs linked to MCF transmission lines are arranged in the R&S configuration. When adjacent SXCs are connected via parallel SMFs instead of an MCF, an SDEMUX (SMUX) is implemented between an ingress (egress) MCF and parallel SMFs as shown in (b).

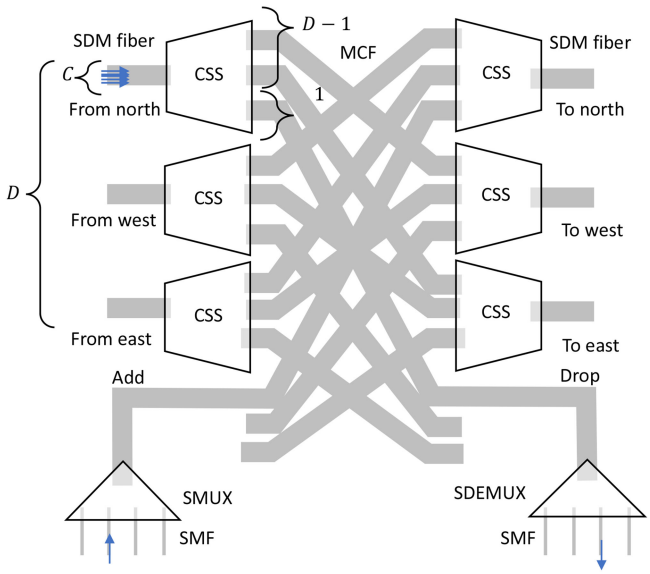

Fig. 13. Architecture of SMUX-type CSS-based SXC (FC/D/CnL/NLC). A line-side CSS used in this architecture is a $1\times D$ CSS whose $D-1$ ports are for through SChs and the remaining port that is linked to an SDEMUX (SMUX) is for local dropping (adding) SChs.

core access (FC), *directional* (D), CnL, and *non-LC* (NLC) features. A line-side CSS used in this architecture is a $1\times D$ CSS whose $D-1$ ports are for through SChs and the remaining port that is linked to an SDEMUX (SMUX) is for local drop (add) SChs. In this architecture, an unused input port on an SMUX can be connected to an unused core with the index associated to the SMUX input port on the egress MCF that the SMUX is linked. Hereafter, we refer to this architecture as the SMUX-type after its client-side structure and categorize its connectivity as FC/D/CnL/NLC.

The required number of CSSs and associated mirrors for this architecture are $2D(=8)$ and $2CD(=512)$, respectively, as summarized in Table V.

2) CS-Type (AC/D/CnL/NLC): The problem related to FC is eliminated by increasing the number of add ports (drop ports) of an egress (ingress) CSS by aC and placing an additional optical device, the CS described in Section IV A, to each add/drop port as shown in Fig. 14. In this architecture, the input (output) of an unused CS can be connected to an unused core on the egress (ingress) MCF that the CS is attached (AC and D). This corresponds to the case where a $1\times K$ WSS and a wavelength-tunable transceiver are introduced into the

TABLE V
REQUIRED DEVICES FOR SMUX-TYPE CSS-BASED SXC (FC/D/CNL/NLC) SHOWN IN FIG. 13

Device		Input/output port count		Number of mirrors per device		Number of devices		Total number of mirrors	
CSS (Line-side)	EoL	$1\times D$	1×8	C	64	$2D$	16	$2CD$	1024
	BoL					↑		↑	

TABLE VI
REQUIRED DEVICES FOR CS-TYPE CSS-BASED SXC (AC/D/CNL/NLC) SHOWN IN FIG. 14

Device		Input/output port count		Number of mirrors per device		Number of devices		Total number of mirrors	
CSS (Line-side)	EoL	$1\times(D-1+\lceil aC\rceil)$	1×23	C	64	$2D$	16	$2CD$	1024
	BoL					↑		↑	
CS	EoL	1×1		1		$2C\lceil aD\rceil$	256	$2C\lceil aD\rceil$	256
	BoL					2		2	

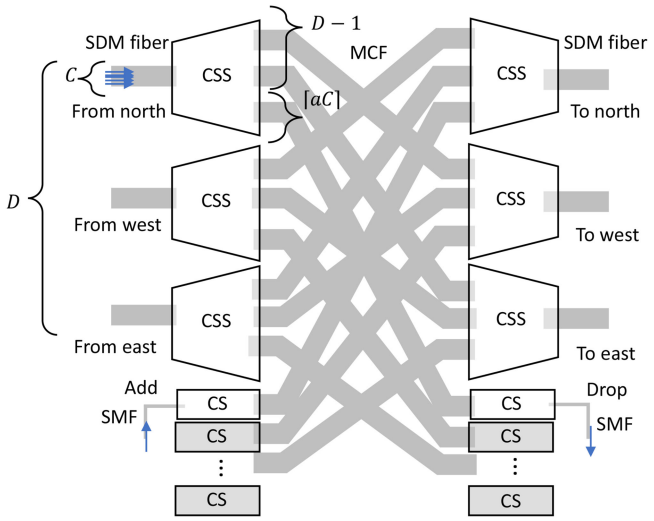

Fig. 14. Architecture of CS-type CSS-based SXC (AC/D/CnL/NLC). The input (output) of an unused CS can be connected to an unused core on the egress (ingress) MCF to which the CS is attached.

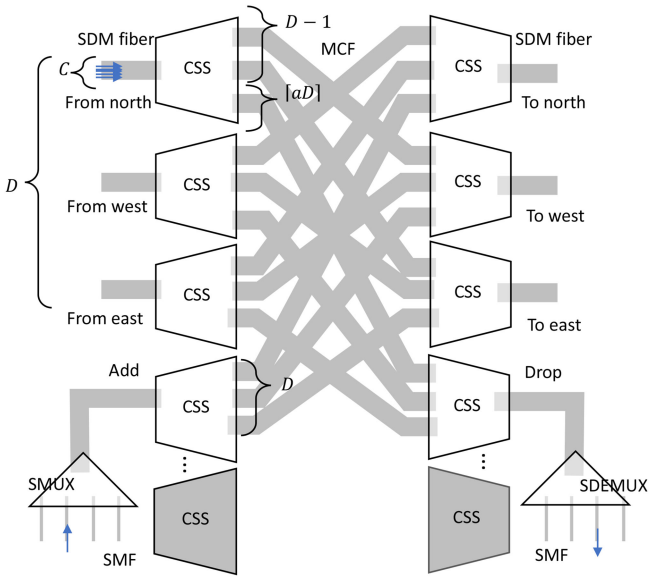

Fig. 15. Architecture of SMUX/CSS-type CSS-based SXC (FC/ND/CnL/NLC). An SMUX and an SDEMUX are attached to client-side CSSs. An unused input (output) port on an SMUX (SDEMUX) can always be connected to an unused core with the index associated to the SMUX input port (SDEMUX output port) on an egress (ingress) MCF.

conventional WSS-based node design in order to achieve ClL connectivity. We refer to this architecture as the CS-type and categorize its connectivity as AC/D/CnL/NLC. The number of add (drop) ports per direction can be expanded by cascading a CSS at an add (drop) port.

The required number of CSSs is the same for BoL and EoL, which is $2D$. The required number of CSs is two at BoL and increases to $2CaD$ at EoL; however, since a CSS only requires one mirror, the number of mirrors at EoL only increases by 25% from the beginning as summarized in Table VI.

3) SMUX/CSS-Type (FC/ND/CnL/NLC): Introducing client -side ingress (egress) CSSs with D output ports for local add (drop) SChs allows us to distribute (aggregate) SChs to each direction (from different directions). This allows us to route remotely SChs across viable paths in the SCN. Fig. 15 shows one possible architecture to support such functionality where an SMUX and an SDEMUX are attached to client-side CSSs. In this architecture, an unused input (output) port on an SMUX (SDEMUX) can always be connected to an unused core with the index associated to the SMUX input port (SDEMUX output port) on an egress (ingress) MCF (FC and ND). We refer to this architecture as the SMUX/CSS-type and categorize its connectivity as FC/ND/CnL/NLC.

The required number of line-side CSSs is the same for BoL and EoL, which is $2D$, while that of client-side CSSs increases from 2 at BoL to $2aD(=4)$ at EoL as summarized in Table VII.

4) CS/CSS^2-Type (AC/ND/CC/NLC): As shown in Fig. 16, introducing aggregation (distribution) CSSs with C output ports each attached to a CS instead of the SMUX/SDEMUX in Fig. 15 allows us to connect an SCh to any core of any egress MCF unless core-contention occurs in the aggregation CSS. In this architecture, the input (output) of an unused CS on an aggregation (distribution) CSS can be connected to an unused core on an egress (ingress) MCF if and only if there is no connection from (to) another CS on the same aggregation (distribution) CSS that

TABLE VII
REQUIRED DEVICES FOR SMUX/CSS-TYPE CSS-BASED SXC (FC/ND/CNL/NLC) SHOWN IN FIG. 15

Device		Input/output port count		Number of mirrors per device		Number of devices		Total number of mirrors	
CSS (Line-side)	EoL	$1\times(D-1+\lceil aD\rceil$	1×9	C	64	$2D$	16	$2CD$	1024
	BoL					↑		↑	
CSS (Client-side)	EoL	$1\times D$	1×8	C	64	$2\lceil aD\rceil$	4	$2C\lceil aD\rceil$	256
	BoL					2		$2C$	128

TABLE VIII
REQUIRED DEVICES FOR CS/CSS2-TYPE CSS-BASED SXC (AC/ND/CC/NLC) SHOWN IN FIG. 16

Device		Input/output port count		Number of mirrors per device		Number of devices		Total number of mirrors	
CSS (Line-side)	EoL	$1\times(D-1+\lceil aD\rceil)$	1×9	C	64	$2D$	16	$2CD$	1024
	BoL					↑		↑	
CSS (Client-side)	EoL	$1\times D$	1×8	C	64	$2\lceil aD\rceil$	4	$2C\lceil aD\rceil$	256
	BoL					2		$2C$	128
CSS (Aggregation)	EoL	$1\times C$	1×64	C	64	$2\lceil aD\rceil$	4	$2C\lceil aD\rceil$	256
	BoL					2		$2C$	128
CS	EoL	1×1		1		$2C\lceil aD\rceil$	256	$2C\lceil aD\rceil$	256
	BoL					2		2	

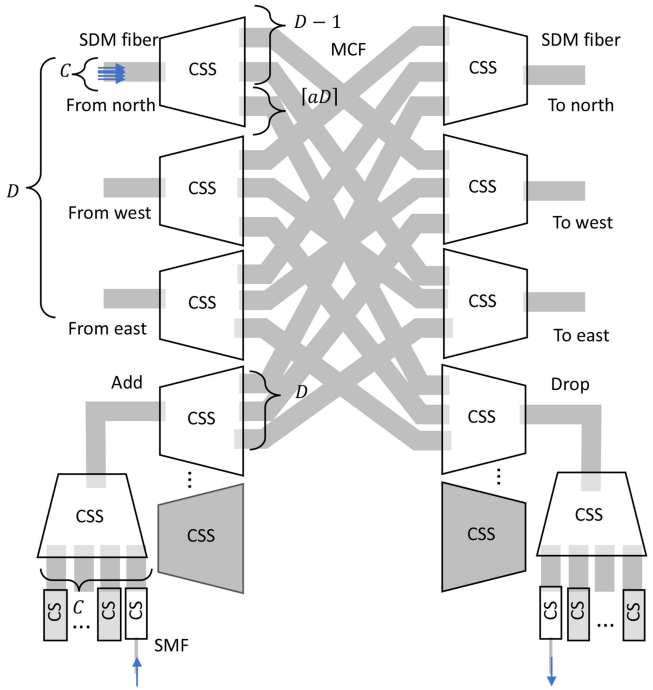

Fig. 16. Architecture of CS/CSS^2-type CSS-based SXC (AC/ND/CC/NLC). Introducing aggregation (distribution) CSSs with C output ports each attached to a CS instead of the SMUX/SDEMUX allows us to connect an SCh to any core of any egress MCF unless core-contention occurs in the aggregation CSS.

already uses the same core (AC, ND, and *core-contention* (CC)). We refer to this architecture as the CS/CSS^2-type and categorize its connectivity as AC/ND/CC/NLC.

The required number of line-side CSSs is the same for BoL and EoL, which is $2D$, while those of client-side CSSs and aggregation CSSs increase from 2 at BoL to $2aD(=4)$ at EoL. On the other hand, the required number of CSs is 2 at BoL and increases to $2CaD$ at EoL. These estimated numbers are summarized in Table VIII.

5) CPS-Type (AC/ND/CnL/NLC): One way to eliminate the CC to achieve highly automated end-to-end SCh provisioning is to introduce another additional optical device, the CPS described in Section IV, to the SXC design. There are two possible architectures for such SXCs relying on a CPS: one requires a high-port count line-side CSS and the other requires aggregation (distribution) CSSs on the client-side to form an $M \times N$ CSS combined with CPSs. Fig. 17 shows the former architecture, which is referred to as the CPS-type and categorize its connectivity as AC/ND/CnL/NLC. Here each MCF port of a $1 \times D$ CPS is linked to an add/drop port of an ingress/egress high port count CSS having a size of $1 \times (D - 1 + aCD)$ $(=1 \times 135)$. In this architecture, an input (output) of an unused CPS can always be connected to any unused core on any egress (ingress) MCF. Such an AC, ND, and CnL SXC solves the core blocking problem and provides flexibility in the SDM layer at the same level that is achieved by a ClL, ND, and CnL ROADM, the so-called CDC-ROADM, in the WDM layer.

The required number of CPSs is 2 at BoL and increases to $2CaD$ at EoL as summarized in Table IX.

6) CPS/CSS-Type (AC/ND/CnL/NLC): Fig. 18 shows another AC, ND, and CnL SXC architecture where $1 \times (aCD/s)$ $(=1 \times 32)$ CSSs and $1 \times D$ $(=1 \times 8)$ CPSs form a $D \times aCD/s$ $(=8 \times 32)$ CSS. This architecture also enables an input (output) of an unused CPS to be connected to any unused core on any egress (ingress) MCF. Although this architecture does not need a high port count CSS and requires only moderate sized CSSs both for a line-side CSS $(=1 \times 11)$ and an aggregation (distribution) CSS $(=1 \times 32)$, it does require a large number of aggregation (distribution) CSSs.

TABLE IX
REQUIRED DEVICES FOR CPS-TYPE CSS-BASED SXC (AC/ND/CNL/NLC) SHOWN IN FIG. 17

Device		Input/output port count		Number of mirrors per device		Number of devices		Total number of mirrors	
CSS (Line-side)	EoL	$1\times(D-1+\lceil aCD\rceil)$	1×135	C	64	$2D$	16	$2CD$	1024
	BoL					↑		↑	
CPS	EoL	$1\times D$	1×8	1		$2C\lceil aD\rceil$	256	$2C\lceil aD\rceil$	256
	BoL					2		2	

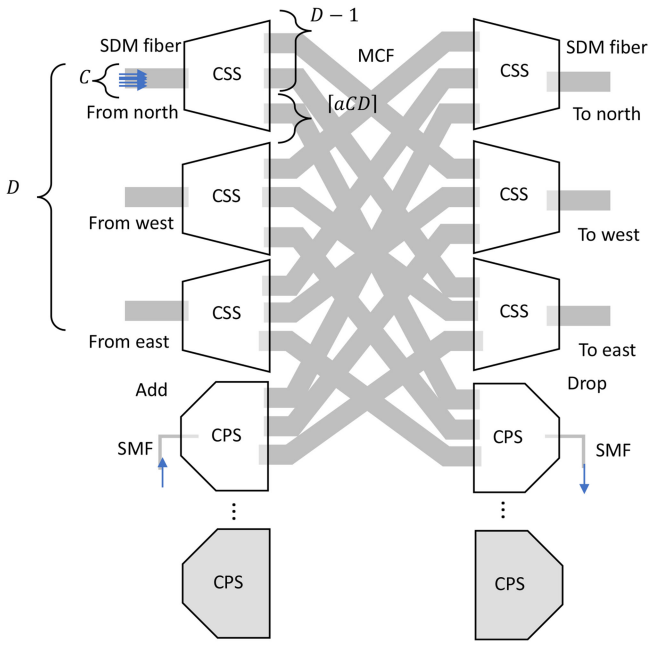

Fig. 17. Architecture of CPS-type CSS-based SXC (AC/ND/CnL/NLC), which requires a high-port count line-side CSS. Each MCF port of a $1 \times D$ CPS is linked to an add/drop port of an ingress/egress high port count CSS having a size of $1 \times (D - 1 + aCD)$.

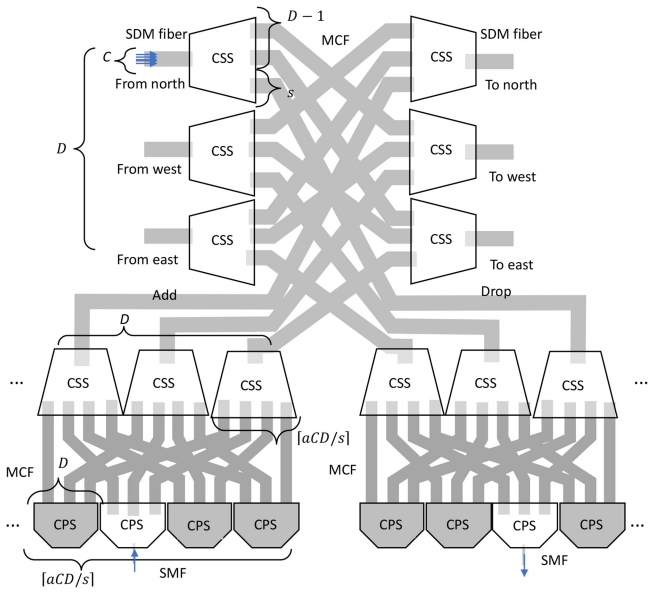

Fig. 18. Architecture of CPS/CSS-type CSS-based SXC (AC/ND/CnL/NLC), which requires aggregation (distribution) CSSs on the client-side to form an $M \times N$ CSS combined with CPSs.

The required number of aggregation CSSs is $2D\ (=16)$ at BoL and increases to $2sD\ (=64)$ at EoL as summarized in Table X.

V. COMPARISON OF SXC ARCHITECTURES

In Sections III and IV, we described a wide variety of SXC architectures based on an MS and CSS. Architectures that have higher degrees of connectivity freedom generally have more complicated structures and incur higher node costs. On the other hand, they yield higher SL utilization efficiency, which decreases the required number of fibers, and/or a higher level of operational automation, which reduces the operational expenditure and increases the service velocity. In this section, we first investigate how the level of LC capability in the SXC architectures affects the total number of assigned SLs in an SCN. We then compare the required numbers of switching mirrors for each SXC architecture using the formulae derived in the previous section, and discuss the advantages and disadvantages of each architecture.

A. Effect of LC Capability on SL Utilization Efficiency

1) Routing and Core Assignment (RCA) Algorithm: In order to investigate how the level of LC capability in the SXC architectures affects the total number of assigned SLs, we developed an RCA algorithm for SCNs [27]. We use $\boldsymbol{C} = \{c_1, c_2, \ldots, c_{|\boldsymbol{C}|}\}$ to denote the ordered set of SLs in each link. The traffic demand set is given by $\boldsymbol{T} = \{t_1, t_2, \ldots, t_{|T|}\}$ where t is determined by source and destination nodes and the requested number of SLs, q. The objectives of the RCA algorithm are to find a route for each demand that is identified by the route, the SL to be used in each link on the route, and the sub-MS at each node on the route by which the SCh is routed (this is the case only for sub-MS-based SXCs) that will minimize the number of SLs that are assigned to at least one demand, N_{SL}, while subject to the following constraints.

- *Common Constraints:* Along with each SCh, an SL for each link must not overlap that of other SChs. A working SCh and its backup SCh must be link- and node-disjoint from each other.
- *Constraints on SCN employing sub-MS-based SXC:* Whenever the ith sub-MS is selected for an SCh, SL c_j where $(i-1)l+1 \le j \le il$ should be assigned along with the SCh. Here, l is the number of sub-SLs that each sub-MS accommodates per link and is indicated by C/s. The working SCh and its backup SCh must be sub-MS-disjoint from each other aside from being link- and node-disjoint.

TABLE X
REQUIRED DEVICES FOR CPS/CSS-TYPE CSS-BASED SXC (AC/ND/CNL/NLC) SHOWN IN FIG. 18

Device		Input/output port count		Number of mirrors per device		Number of devices		Total number of mirrors	
CSS (Line-side)	EoL	$1\times(D-1+s)$	1×11	C	64	$2D$	16	$2CD$	1024
	BoL					↑		↑	
CSS (Aggregation)	EoL	$1\times(\lceil aCD/s\rceil)$	1×32	C	64	$2\lceil sD\rceil$	64	$2sCD$	4096
	BoL					$2D$	16	$2DC$	1024
CPS	EoL	$1\times D$		1		$2s\lceil aCD/s\rceil$	256	$2s\lceil aCD/s\rceil$	256
	BoL					2		2	

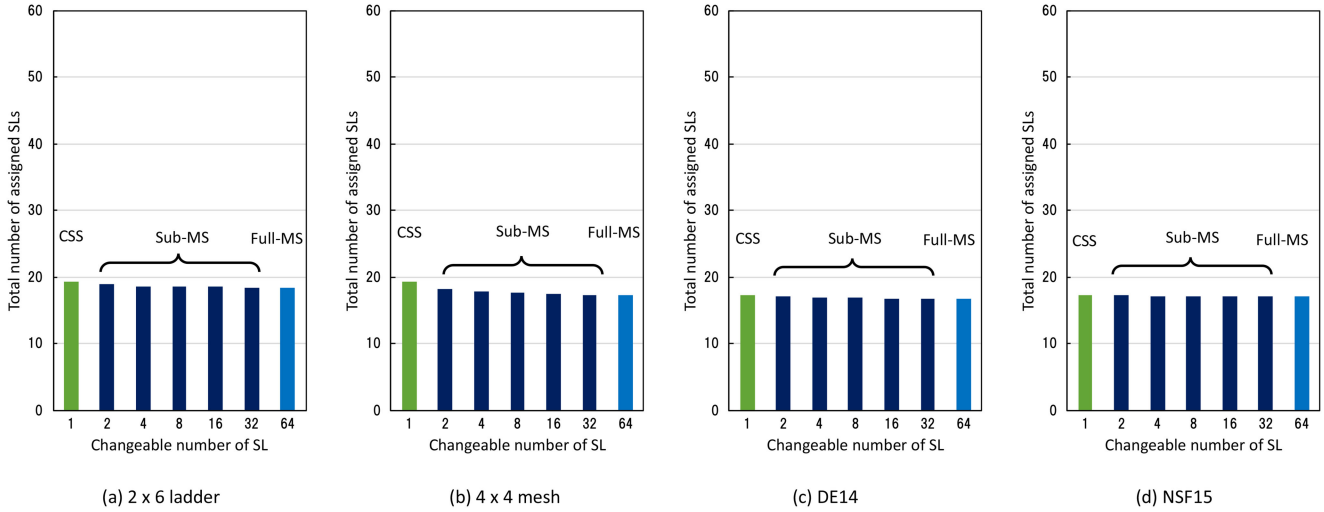

Fig. 19. Total number of assigned SLs for unprotected traffic demands. The changeable number of SLs of one corresponds to the case of a CSS-based CnL SXC and 64 corresponds to the case of a full-MS based or a Clos-network based SXC. Values of 2, 4, 8, 16, and 32 correspond to the cases of a sub-MS based SXC where each sub-MS accommodates l sub-SLs ($l = 2,\ 4,\ 8, 16, 32$) per link.

- *Constraints on SCN employing CSS-based SXC:* Each SL comprising an SCh must have the same SL index.

When a connection demand arrives, the RCA algorithms are aimed at finding a route so that N_{SL} is minimized after the SCh is established.

2) Simulation Results: Figs. 19 and 20 show the simulation results on the total number of assigned SLs, N_{SL}, in an SCN as a function of the changeable number of SLs, n_{LC}, when an unprotected SCh (Fig. 19) and working and backup SChs (Fig. 20) are assigned to network models with a 4×4 mesh (16 nodes, 24 links, averaged node degree of 3), a 2×6 ladder (12 nodes, 16 links, averaged node degree of 2.8), DE14 (14 nodes, 23 links, averaged node degree of 3.3), and NSF15 (15 nodes, 23 links, averaged node degree of 3.1), respectively. Here, we assume 64 SLs per link and full-mesh *incremental* traffic demands each requiring one SL ($q = 1$). The changeable number of SLs, n_{LC}, of one corresponds to the case of a CSS-based CnL SXC and 64 corresponds to the case of a full-MS based or a Clos-network based SXC, respectively. Values of 2, 4, 8, 16, and 32 correspond to the cases of a sub-MS based SXC where each sub-MS accommodates $l\ (=C/s)$ sub-SLs ($l = 2,\ 4,\ 8, 16, 32$) per link. Since N_{SL} depends on the order of the demand to be served and the dependency differs based on the applied network topologies, the averaged N_{SL} over 10,000 randomly created order sets is employed for the performance evaluation for an incremental traffic demand case.

Fig. 19 shows that for the unprotected case, N_{SL} gradually increases as n_{LC} decreases due to the lower LC capability; however, the increment in N_{SL} is small ($<12\%$ for a 4×4 mesh, $<5\%$ for a 2×6 ladder, $<3\%$ for DE14, and $<1\%$ for NSF15). It should be noted that a similar tendency is also observed in wavelength conversion in conventional WDM networks [33]. Fig. 20 shows that for the $1\ +\ 1$ protected case, N_{SL} for the sub-MS with a larger l increases due to the sub-MS-disjoint constraint resulting in the optimum values for l and the optimum sub-MS size. However, the difference in N_{SL} among SXCs based on a CSS, sub-MSs with a moderate size of l (≤ 8), and a full-MS or a clos-network is still small ($<9\%$ for a 4×4 mesh, $<5\%$ for a 2×6 ladder, $<1\%$ for DE14, and $<3\%$ for NSF15).

B. Required Numbers of Switching Mirrors and Internal Fibers

In general, different network operators or over-the-top players should have different business circumstances and may have different preferences for their optical transport networks. Based on the observation regarding the effect of the LC capability

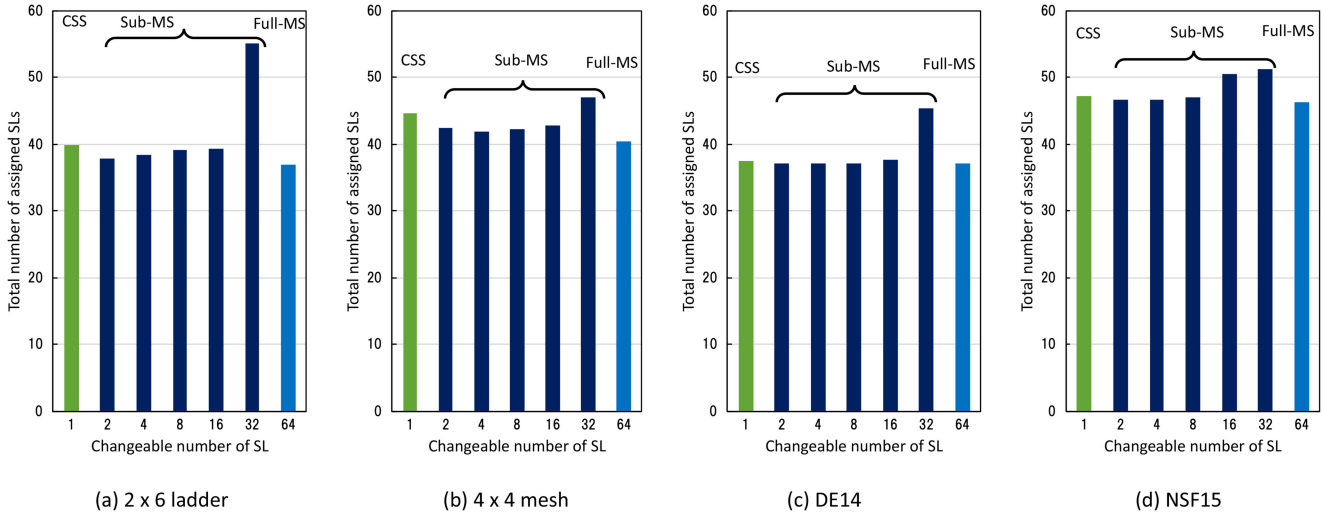

Fig. 20. Total number of assigned SLs for $1+1$ protected traffic demands. The changeable number of SLs of one corresponds to the case of a CSS-based CnL SXC and 64 corresponds to the case of a full-MS based or a Clos-network based SXC. Values of 2, 4, 8, 16, and 32 correspond to the cases of a sub-MS based SXC where each sub-MS accommodates l sub-SLs ($l = 2,\ 4,\ 8, 16, 32$) per link.

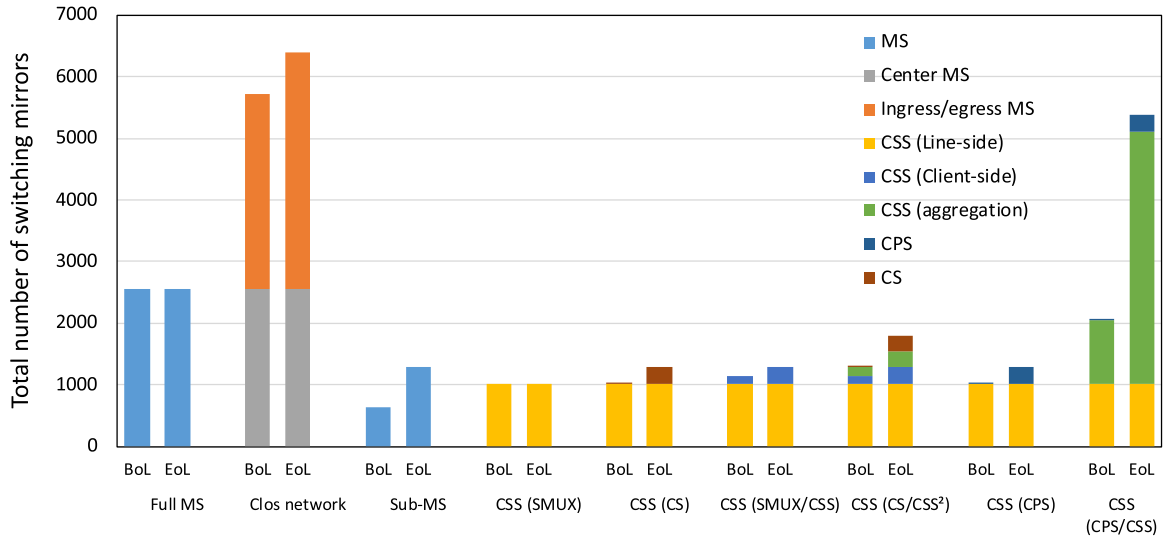

Fig. 21. Number of required switching mirrors at BoL and EoL for SXCs based on a full MS, Clos network, sub-MS, and CSS.

described in the previous sub-section and the results of the required number of optical devices and switching mirrors, we will discuss the advantages and disadvantages of each architecture described in Sections III and IV. Fig. 21 shows the required total number of switching mirrors for SXCs based on a full-MS, Clos network, sub-MS, SMUX-type CSS, CS-type CSS, SMUX/CSS-type CSS, CS/CSS^2-type CSS, CPS-type CSS, and CS/CSS-type CSS, respectively. Fig. 22 shows the required total number of internal fibers at EoL for the SXCs. Here, internal fibers include client-side input/output SMFs. Formulas for the necessary number of internal SMFs and MCFs for the SXC architectures are summarized in Table XI. These numbers can be used as a common index for roughly estimating the total costs of the SXC architectures employing different technologies.

1) Lane Change Aspect: Since LC in the spatial domain, which can be performed using an MS, is easier to implement than in the wavelength domain, which requires expensive optical-to-electrical-to-optical conversion, introducing a SXC may be a great opportunity to enhance the degree of connectivity freedom in the optical domain. Among the SXC architectures, the full-MS based and the Clos-network based SXC architectures are strict-sense non-blocking, and so provide the full LC capability. Fig. 21 shows that this connectivity flexibility is at the expense of a much larger number of switching mirrors and consequently a higher node cost when compared to sub-MS based or CSS-based SXC architectures, which have a limited LC capability.

There are no clear indications yet, but if future traffic demands become more dynamic and if the fragmentation of SLs caused by frequent setting-up and tearing-down of SChs reduces the SL utilization efficiency to an unacceptable level in an SCN employing SXCs with limited LC capabilities, the full-MS based and the Clos-network based non-blocking SXC architectures

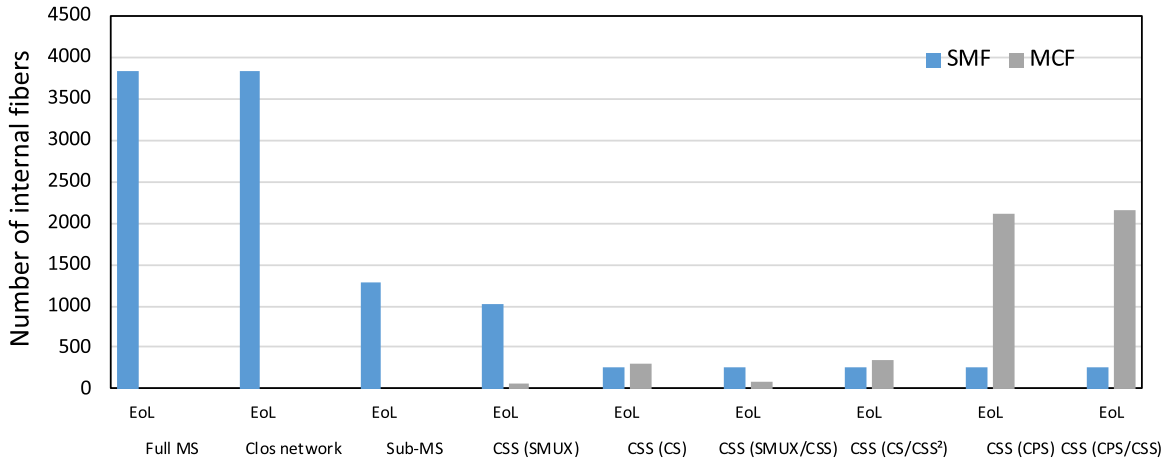

Fig. 22. Number of required internal fibers at EoL for SXCs based on a full MS, Clos network, sub-MS, and CSS. Internal fibers include client-side input/output SMFs. Formulas for the necessary number of internal SMFs and MCFs for the SXC architectures are summarized in Table XI.

TABLE XI
NECESSARY NUMBER OF INTERNAL SMFS AND MCFS

Architecture	Number of SMFs		Number of MCFs		Number of total fibers	
Full-MS	$6(1+a)$CD	3840	-	0	$6(1+a)$CD	3840
Clos network	$6(1+a)$CD	3840	-	0	$6(1+a)$CD	3840
Sub-MS	$2(1+a)$CD	1280	-	0	$2(1+a)$CD	1280
CSS (SMUX)	$2CD$	1024	D^2+D	72	$D^2+(1+2C)D$	1096
CSS (CS)	$2aCD$	256	$D(D-1+aC)+aCD$	312	$D(D-1+aC)+3aCD$	568
CSS (SMUX/CSS)	$2aCD$	256	$D(D-1+aD)+aD^2+2aD$	92	$D(D-1+aD)+aD^2+2aD$+$2aCD$	348
CSS (CS/CSS²)	$2aCD$	256	$D(D-1+aD)+aD^2+2aD+2aCD$	348	$D(D-1+aD)+aD^2+2aD$+$4aCD$	604
CSS (CPS)	$2aCD$	256	$D(D-1+aCD)+aCD^2$	2104	$D(D-1+aCD)+aCD^2$+$2aCD$	2360
CSS (CPS/CSS)	$2aCD$	256	$D(D-1+s)+sD+2aCD^2$	2168	$D(D-1+s)+sD+2aCD^2$+$2aCD$	2424

may be preferable. The full-MS based architecture requires only half the total number of switching mirrors than the Clos-network based architecture, while it should implement fault-dependent link and equipment protection mechanisms, which need a fault localization process and may require longer recovery times [24]. If an ultra-high port count MS is difficult to manufacture for some technical reason, the Clos-network based architecture may be the only option. Fig. 22 shows that among the SXC architectures, these two non-blocking SXC architectures require the largest amount of internal SMF wiring.

On the other hand, if future traffic demands for transport networks remain static or incremental similar to most current traffic demands, the few percent increase in N_{SL} for sub-MS based and CSS-based SXC architectures exhibited in Figs. 19 and 20 may be acceptable for a less expensive node cost as shown in Fig. 21. Except for the SXC based on the CPS/CSS-type CSS, the total number of switching mirrors needed is not very different among sub-MS based and CSS-based SXC architectures.

2) SDM Link Type Aspect: The most significant difference between the two options in the latter scenario (*i.e.,* future traffic demands will remain static or incremental), sub-MS based and CSS-based SXC architectures, is whether it is inherently MCF compatible. If we compare Fig. 7 with Figs. 13–18, it is apparent that a sub-MS is an SMF-based optical switch and thus needs SDEMUXs/SMUXs that serve as interfaces between MCF transmission lines and sub-MSs resulting in a larger number of internal SMF wiring. Since output (input) SMFs of an SDEMUX (SMUX) are partitioned into s SMF groups with continuous SMF indexes where each SMF group is accommodated in an associated sub-MS, the complexity of SMF wiring may be mitigated by replacing a SMF group with a ribbon SMF. On the other hand, a CSS is a MCF compatible device, which does not require a SDEMUX/SMUX. The internal wiring is done using MCFs except for client-side input/output SMFs, which basically results in a smaller number of internal fibers and yields better installation workability. The reasons why large numbers of internal fibers are required in SXC architectures based on the SMUX-type CSS, CPS-type CSS, and CS/CSS-type CSS are explained later.

3) Any-Core Access Aspect: The fewest switching mirrors needed at the EoL is attained by an SXC based on the SMUX-type CSS shown in Fig. 13. However, in this architecture, since an input (output) port of an SMUX (SDEMUX) is tied to a specific core of a specific direction (FC and ND), Each SMUX

(SDEMUX) should have input (output) SMF ports for all C cores from the beginning in order to prepare for an unpredictable core index needed for a future demand. Due to this connectivity restriction, changing the core and direction requires a manual rewiring at the site.

In conventional WDM networks, ClL functionality that enables any wavelength to be added/dropped at any port is achieved by introducing a WSS and a sophisticated wavelength tunable transceiver. In an SCN, corresponding AC functionality can be achieved by employing a simple CS as shown in Fig. 14. Operators can remotely reconfigure cores without site visits by controlling a CS. Since a CS needs only one switching mirror, the increase in the number of switching mirrors for an SXC based on the CS-type CSS is 25% resulting in the same total number with that based on a sub-MS at EoL. The number of necessary internal fibers is reduced to 44% of that for the sub-MS based SXC architecture. Further reduction to 24% can be obtained if a CS is equipped inside a transceiver, which has input/output MCFs, similar to a transceiver used in current WDM networks that has built-in wavelength tunability. Due to its simple structure and potential low node cost, the SXC architecture based on the CS-type CSS may be suitable for MCF ring networks in the metro-core tier.

4) Non-Directional Aspect: The CS/CSS^2-type CSS achieves AC and ND connectivity that enable operators to route remotely SChs across a viable path in the SCN, which is beneficial in quickly adapting to changing service requirements as well as in providing highly-resilient SCh restoration. In addition to CSs, this architecture requires client-side CSSs and aggregation (distribution) CSSs and the total number of switching mirrors needed at EoL increases by 40% compared to SXCs based on a sub-MS and CS-type CSSs. The necessary number of internal fibers is reduced to 47% that for the sub-MS based SXC architecture and further reduction to 27% can be obtained if a CS is equipped inside a transceiver. Due to its ND feature, the SXC architecture based on the CS/CSS^2-type CSS may be suitable for MCF mesh networks in regional and backbone tiers.

5) Core-Contention Aspect: The CPS-type and CS/CSS-type CSSs are able to eliminate the CC observed in the CS/CSS^2-type CSS to achieve highly automated end-to-end SCh provisioning. Although an SXC architecture based on the CPS-type CSS only requires a 25% increase in the total number of switching mirrors, it requires high port count line-side CSSs (1×135) and may incur some manufacturing problems. On the other hand, an SXC architecture based on the CS/CSS-type CSS requires moderate sized CSSs. Although, it requires a considerable number of CSSs on the client side, the total number of switching mirrors at BoL is still less than that for full-MS based and Clos-network based SXCs and the total number of switching mirrors at EoL is less than that for a Clos-network based SXC. The necessary numbers of internal fibers for these two architectures are approximately 65% that for the Clos-network based architecture, but still much larger than that for the sub-MS based architecture. This is due to the poor utilization of SL resources in the add/drop MCFs for the SXC based on the CPS-type CSS and in the MCFs inside the $M \times N$ CSSs for the SXC based on the CPS/CSS-type CSS.

VI. Conclusion

In this paper, we discussed a wide variety of SXCs as a key enabler to achieve ultra-high capacity, long reach, and cost-effective SCNs toward the forthcoming SDM era, from the viewpoints of connection flexibility and architectural complexity. Novel SXC architectures based on sub-MSs and CSSs were described and formulas were derived for each SXC architecture that give the required number of optical devices, switching mirrors, and internal fiber connections. Using the formulation, these architectures were compared with traditional SXC architectures based on a high-port count full-MS pair and a Clos-network.

The important question is which SXC architectures will achieve techno-economical validity in future SCNs. However, this depends on many factors such as traffic patterns (dynamic or incremental), fiber types (parallel SMFs or MCF), maturity of support technologies (optical amplifiers, optical switches, SMUX/SDEMUX, etc.) in future SCNs, and there is no clear technological forecast to these factors at this time. For example, when optical bypass technology was developing, it was quite clear that wavelengths are multiplexed in a core of a standard SMF and an erbium-doped fiber amplifier (EDFA) optically amplified all of the wavelengths in the core at once. This apparently made WSS-based ROADMs/WXCs more preferable over MS-based WXCs because WSSs do not require each wavelength to be demultiplexed into an individual SMF. In contrast, it is not clear at this moment whether traffic in the near future will be carried by parallel SMFs, MCFs, or both.

Therefore, our answer must be conditional at this moment. According to our analysis, if MCFs and EDFAs with an MCF input/output (no matter how it comprises a micro EDFA array, a cladding pumping MCF EDFA, or whatever) will be widely deployed and demands will remain quasi-static, a CSS-based SXC will be the first choice because it is inherently MCF compatible and requires less internal wiring. Considering the necessary number of switching mirrors and internal fiber connections, SXCs based on the CS-type CSS and CS/CSS^2 type CSS may be suitable for metro-core ring networks and regional and backbone mesh networks, respectively. An SXC based on a sub-MS will also be a good choice due to its small number of necessary switching mirrors, and will be more competitive if future SDM links comprise parallel SMFs, although a CSS-based SXC may still remain competitive. SXCs based on a Clos network may find a place to play a major role if dynamic huge data transfer services that can validate their highest node cost materialize, although there are no clear indications.

Whichever SXC architecture that will be put to practical use, there is no doubt that future SCNs will need a cost-effective and low-loss SXC itself to form an ultra-high capacity HOXC that can accommodate a wide variety of data traffic in a spatially and spectrally efficient manner.

References

[1] P. J Winzer and D. T Neilson, "From scaling disparities to integrated parallelism: A decathlon for a decade," *J. Lightw. Technol.*, vol. 35, no. 5, pp. 1099–1115, Mar. 2017.

[2] P. J. Winzer, D. T. Neilson, and A. R. Chraplyvy, "Fiber-optic transmission and networking: The previous 20 and the next 20 years," *Opt. Express*, vol. 26, no. 18, pp. 24190–24239, 2018.

[3] P. J. Winzer, "Scaling optical fiber networks: Challenges and solutions," *Opt. Photon. News*, vol. 26, no. 3, pp. 28–35, Mar. 2015.
[4] D. M. Marom and M. Blau, "Switching solutions for WDM- SDM optical networks," *IEEE Commun. Mag.*, vol. 53, no. 2, pp. 60–68, Feb. 2015.
[5] D. M. Marom *et al.*, "Survey of photonic switching architectures and technologies in support of spatially and spectrally flexible optical networking [Invited]," *J. Opt. Commun. Netw.*, vol. 9, no. 1, pp. 1–26, 2017.
[6] M. D. Feuer *et al.*, "ROADM system for space division multiplexing with spatial superchannels," in *Proc. Opt. Fiber Commun. Conf.*, 2013, Paper PDP5B.8.
[7] L. E. Nelson *et al.*, "Spatial superchannel routing in a two-span ROADM system for space division multiplexing," *J. Lightw. Technol.*, vol. 32, no. 4, pp. 783–789, Feb. 2014.
[8] Y. Iwai, H. Hasegawa, and K. Sato, "A large-scale photonic node architecture that utilizes interconnected OXC subsystems," *Opt. Express*, vol. 21, no. 1, pp. 478–487, 2013.
[9] R. Hashimoto *et al.*, "First demonstration of subsystem-modular optical cross-connect using single-module 6×6 wavelength-selective switch," *J. Lightw. Technol.*, vol. 36, no. 7, pp. 1435–1442, Apr. 2018.
[10] A. A. M. Saleh, "Transparent optical networking in backbone networks," in *Proc. Opt. Fiber Commun. Conf.*, 2000, Paper ThD7.
[11] E. Modiano and A. Narula-Tam, "Mechanisms for providing optical bypass in WDM-based networks," *SPIE Opt. Netw. Mag.*, vol. 1, no. 1, pp. 9–16, Jan. 2000.
[12] D. Klonidis *et al.*, "Spectrally and spatially flexible optical network planning and operations," *IEEE Commun. Mag.*, vol. 53, no. 2, pp. 69–78, Feb. 2015.
[13] R. Proietti *et al.*, "3D elastic optical networking in the temporal, spectral, and spatial domains," *IEEE Commun. Mag.*, vol. 53, no. 2, pp. 79–87, Feb. 2015.
[14] K. Harada, K. Shimizu, and T. Kudou, "Hierarchical optical path cross-connect systems for large scale WDM networks," in *Proc. Opt. Fiber Commun./IOOC*, 1999, vol. 2, pp. 356–358.
[15] M. Jinno, J. Kani, and K. Oguchi, "Ultra-wide-band WDM networks and supporting technologies," in *Proc. NOC' 99, Core Netw. Netw. Manage.*, 1999, pp. 90–97.
[16] A. A. M. Saleh and J. M. Simmons, "Architectural principles of optical regional and metropolitan access networks," *J. Lightw. Technol.*, vol. 17, no. 12, pp. 2431–2448, Dec. 1999.
[17] X. Cao, V. Anand, and C. Qiao, "Framework for waveband switching in multigranular optical networks: Part I-Multigranular cross-connect architectures," *J. Opt. Netw.*, vol. 5, no. 12, pp. 1043–1055, 2006.
[18] K. Ishii *et al.*, "An ultra-compact waveband cross-connect switch module to create cost-effective multi-degree reconfigurable optical node," in *Proc. Eur. Conf. Exhib. Opt. Commun.*, 2009, Paper 4.2.2.
[19] M. Cvijetic, I. B. Djordjevic, and N. Cvijetic, "Dynamic multidimensional optical networking based on spatial and spectral processing," *Opt. Express*, vol. 20, no. 8, pp. 9144–9150, 2012.
[20] N. Amaya *et al.*, "Fully-elastic multi-granular network with space/frequency/time switching using multi-core fibres and programmable optical nodes," *Opt. Express*, vol. 21, no. 7, pp. 8865–8872, 2013.
[21] G. M. Saridis *et al.*, "Experimental demonstration of a flexible filterless and bidirectional SDM optical metro/inter-DC network," in *Proc. Eur. Conf. Opt. Commun.*, 2016, Paper M.1.F.3.
[22] A. C. Jatoba-Neto, D. A. A. Mello, C. E. Rothenberg, S. Ö. Arik, and J. M. Kahn, "Scaling SDM optical networks using full-spectrum spatial switching," *IEEE/OSA J. Opt. Commun. Netw.*, vol. 10, no. 12, pp. 991–1004, Dec. 2018.
[23] M. Jinno, "Spatial channel network (SCN) architecture employing growable and reliable spatial channel cross-connects toward massive SDM era," in *Proc. Int. Conf. Photon. Switching Comput.*, Sep. 2018, Paper Fr3C.5.
[24] M. Jinno, "Spatial channel network (SCN): Opportunities and challenges of introducing spatial bypass toward massive SDM era [Invited]," *J. Opt. Commun. Netw.*, vol. 11, no. 3, pp. 1–14, 2019.
[25] M. Jinno, K. Yamashita, and Y. Asano, "Architecture and feasibility demonstration of core selective switch (CSS) for spatial channel network (SCN)," in *Proc. OECC/PSC*, Jul. 2019, Paper WA2-3.
[26] M. Jinno, T. Kodama, and T. Ishikawa, "Five-core 1×6 core selective switch and its application to spatial channel networking," in *Proc. Opt. Fiber Commun.*, 2020, Paper M3F.3.
[27] M. Jinno, T. Kodama, T. Ishikawa, and Y. Asano, "Demonstration of spatial channel networking using two types of hierarchical optical cross-connects," in *Proc. Eur. Conf. Opt. Commun.* 2019, Paper Th1A.6.
[28] M. Jinno and Y. Asano, "Required link and node resource comparison in spatial channel networks (SCNs) employing modular spatial channel cross-connects (SXCs)," in *Proc. Opt. Fiber Commun.*, Mar. 2019, Paper M1A.1.
[29] M. Jinno, "Added value of introducing spatial bypass into WDM/SDM networks: Gaussian-noise model analysis for spatially-bypassed and spectrally-groomed optical channels," in *Proc. Eur. Conf. Opt. Commun.*, Sep. 2018, Paper We3D.6.
[30] P. Poggiolini, G. Bosco, and A. Carena, "The LOGON strategy for low-complexity control plane implementation in new-generation flexible networks," in *Proc. Opt. Fiber Commun. Conf.*, 2013, Paper OW1H.3.
[31] O. Shimakawa, M. Shiozaki, T. Sano, and A. Inoue, "Pluggable fan-out realizing physical-contact and low coupling loss for multi-core fiber," in *Proc. Opt. Fiber Commun. Conf.*, 2013, Paper OM3I.2.
[32] K. Watanabe and T. Saito, "Compact fan-out for 19-core multicore fiber, with high manufacturability and good optical properties," in *Proc. Opto-Electronics Commun. Conf.*, 2015.
[33] B. Mukherjee, *Optical WDM Networks*. Berlin, Germany: Springer, 2006.

Masahiko Jinno (Fellow, IEEE) received the B.E. degree and M.E. degree in electronics engineering from Kanazawa University, Ishikawa, Japan, in 1984 and 1986, respectively. He received the Ph.D. degree in engineering from Osaka University, Osaka, Japan, in 1995 for his work on ultra-fast optical signal processing based on nonlinear effects in optical fibers.

He is currently working as a Professor of the Faculty of Engineering and Design with Kagawa University, Takamatsu, Japan. Prior to joining Kagawa University in October 2012, he was a Senior Research Engineer and Supervisor with Nippon Telegraph and Telephone (NTT) Network Innovation Laboratories, NTT Corporation conducting pioneering research on spectrum- and energy-efficient elastic optical networks (EONs). From 1993 to 1994, he was a Guest Scientist with the National Institute of Standards and Technology, Boulder, CO, USA. He authored or co-authored more than 180 peer-reviewed journal and conference papers in the fields of ultra-fast optical signal processing for high-capacity optical time division multiplexed transmission systems, optical sampling and optical time-domain reflectometry, ultra-wideband DWDM transmission systems in the L-band and S-band, ROADM systems, GMPLS and application-aware optical networking, EONs, and SDM networks. His current research interests include architecture, design, management, and control of optical networks, optical transmission systems, optical cross-connects, optical switches, rate- and format-flexible optical transponders.

Prof. Jinno is a Fellow of the Institute of Electronics, Information and Communication Engineers (IEICE) and a Member of the Optical Society of America. He received the Young Engineer's Award in 1993, the Best Tutorial Paper Award in 2011, the Best Paper Award in 2012, the Achievement Award in 2017, and the Milestone Certificate in 2017 from the IEICE, the Best Paper Awards from the 1997, 1998, 2007, and 2019 Optoelectronics and Communications Conferences, the Best Paper Award from the 2010 ITU-T Kaleidoscope Academic Conference, and the Outstanding Paper Award in 2013 from the IEEE Communications Society Asia-Pacific Board.